B-Cell-Targeted 3DNA Nanotherapy Against Indoleamine 2,3-Dioxygenase 2 (IDO2) Ameliorates Autoimmune Arthritis in a Preclinical Model

Clinical Pathology
Volume 13: 1–8

DOI: 10.1177/2632010X20951812

Lauren MF Merlo[1], Jessica Bowers[2], Tony Stefanoni[2], Robert Getts[2] and Laura Mandik-Nayak[1]

[1]Lankenau Institute for Medical Research, Wynnewood, PA, USA. [2]Genisphere, LLC, Hatfield, PA, USA.

ABSTRACT: The tryptophan catabolizing enzyme indoleamine 2,3-dioxygenase 2 (IDO2) has been identified as an immunomodulatory agent promoting autoimmunity in preclinical models. As such, finding ways to target the expression of IDO2 in B cells promises a new avenue for therapy for debilitating autoimmune disorders such as rheumatoid arthritis. IDO2, like many drivers of disease, is an intracellular protein expressed in a range of cells, and thus therapeutic inhibition of IDO2 requires a mechanism for targeting this intracellular protein in specific cell types. DNA nanostructures are a promising novel way of delivering small molecule drugs, antibodies, or siRNAs to the cytoplasm of a cell. These soluble, branched structures can carry cell-specific targeting moieties along with their therapeutic deliverable. Here, we examined a 3DNA nanocarrier specifically targeted to B cells with an anti-CD19 antibody. We find that this 3DNA is successfully delivered to and internalized in B cells. To test whether these nanostructures can deliver an efficacious therapeutic dose to alter autoimmune responses, a modified anti-IDO2 siRNA was attached to B-cell-directed 3DNA nanocarriers and tested in an established preclinical model of autoimmune arthritis, KRN.g7. The anti-IDO2 3DNA formulation ameliorates arthritis in this system, delaying the onset of joint swelling and reducing total arthritis severity. As such, a 3DNA nanocarrier system shows promise for delivery of targeted, specific, low-dose therapy for autoimmune disease.

KEYWORDS: 3DNA, arthritis, indoleamine 2,3-dioxygenase 2, IDO2, autoimmunity

RECEIVED: July 16, 2020. **ACCEPTED:** July 30, 2020.

TYPE: Original Research

FUNDING: The author(s) disclosed receipt of the following financial support for the research, authorship, and/or publication of this article: This work was funded by the Lankenau Medical Center Foundation, the Zuckerman Family Autoimmune Disorder Research Fund at Lankenau Medical Center, and Main Line Health.

DECLARATION OF CONFLICTING INTERESTS: The author(s) declared the following potential conflicts of interest with respect to the research, authorship, and/or publication of this article: J.B. is Director of Academic Collaborations and Marketing Communications, T.S. is a Research and Development Scientist, and R.G. is Founder and Chief Scientific Officer of Genisphere LLC, the commercial manufacturer of 3DNA. L.M.-N. and L.M.F.M. declare no conflict of interest.

CORRESPONDING AUTHOR: Laura Mandik-Nayak, Lankenau Institute for Medical Research, 100 East Lancaster Avenue, Wynnewood, PA 19096, USA.
Email: mandik-nayakl@mlhs.org

Introduction

Autoimmune disorders are a significant public health issue, with an estimated prevalence in the population of 4.5%.[1] These disorders are characterized by a breakdown in immunological tolerance, leading to attack on the body's healthy cells, tissue, or organs. The most common autoimmune disorders include type I diabetes, Graves' disease, Hashimoto's thyroiditis, celiac disease, and rheumatoid arthritis (RA). Indeed, autoimmune disorders are among the leading causes of morbidity in the United States and collectively are among the top 10 causes of death for women under age 65.[2,3] Rheumatoid arthritis alone affects an estimated 1% of the population and, like other autoimmune diseases, can lead to diminished quality of life and significant loss of income.[4-6] Treatment for autoimmunity has generally focused on therapies that dampen the immune system as a whole such as corticosteroids or non-steroidal anti-inflammatory drugs (NSAIDs). These require long-term use at high doses, and there has been a push to develop more specific therapies, including disease-modifying anti-rheumatic drugs (DMARDs) and biologic response-modifying drugs.[7-10] Unfortunately, these directed therapies are only effective in a proportion of patients and are associated with significant side effects, including injection site reactions, toxicities associated with long-term use, and infection risk.[9,11] In addition, most of the biologic therapies for autoimmunity have either cell-surface or secreted targets. Although intracellular targets have been identified, they are harder to pursue therapeutically, particularly if there are not good specific small molecule inhibitors available or if the exact function of the potential target is not fully elucidated. Thus, new therapies for rheumatoid arthritis and other autoimmune disorders that can be directed to intracellular proteins with minimal side effects are needed.

One such promising intracellular target for autoimmune disease is the enzyme indoleamine 2,3-dioxygenase 2 (IDO2). Using genetic knockouts, we have previously shown that elimination of IDO2 reduces autoimmune arthritis in the well-established KRN.g7 murine model system of disease.[12] Further studies have established that elimination of IDO2 specifically from B cells is enough to recapitulate the reduction in arthritis seen with IDO2 ko KRN.g7 mice, thus establishing B-cell-expressed IDO2 as a pro-inflammatory mediator of autoimmune disease initiation, progression, and severity.[12-14] Despite clear empirical evidence for the role of IDO2 in driving autoimmunity, little is known about its function. IDO2 is 1 of 2 known IDO enzymes (IDO1 and IDO2) that, along with the liver enzyme tryptophan 2, 3-dioxygenase (TDO), catabolize the amino acid tryptophan. IDO1, the better studied of the two, is also associated with regulatory T-cell function and is an important mediator of immune escape associated with cancer development.[15-18] Unlike IDO2, IDO1's role in the autoimmune

response is unclear, with some studies suggesting a regulatory function,[19-22] while others suggest a pro-inflammatory role[23-25] or no role at all.[12,26] Although several small molecule inhibitors of IDO1 have been developed, small molecules that specifically inhibit IDO2 have yet to be identified.[27,28] Our data suggest a therapeutic strategy specifically directed against IDO2, rather than IDO1 or the broader IDO pathway, could be of great benefit to clinical disease management and has the potential to reduce side effects associated with targeting multiple members of the immunomodulatory tryptophan catabolic pathway.

As IDO2 is an intracellular protein and not known to be secreted or to be expressed on the cell surface, targeting this regulatory molecule is challenging. Prior work in preclinical models suggests that it may be possible to target IDO2 and other intracellular antigens with antibody therapies.[29] However, a broadly applicable, easily adaptable therapy for intracellular antigens is urgently needed. siRNA therapies have shown promise in preclinical settings, but complications with targeting and delivery of siRNA to specific cells have made siRNA therapy less translatable for general clinical use.[30] The use of DNA nanostructures as delivery systems overcomes many of these limitations.[31] 3DNA nanocarriers are flexible, branched, soluble nanostructures made from DNA, that can be customized with highly specific antibodies directed to the cell type of interest, while carrying small molecules, antibodies, or siRNA to their intracellular targets. Various 3DNA formulations have been shown to specifically engage relevant cell populations, escape degradation in the endosomal compartment of the target cells, and have limited accumulation in clearance organs such as the liver.[32] These antibody-coupled 3DNA molecules have long-term stability in buffers and a half-life of at least 26 hours in serum.[32] In preclinical models, these 3DNA-based treatments have been successful in delivery of siRNA against HuR in ovarian cancers, antibodies against ICAM-1 in lung disease, cytotoxic doxorubicin directed to myofibroblast precursors in the eye associated with vision impairment, and a Wnt signaling agonist to microglia in the brain.[32-36]

Here, we are extending this technology as an approach to treat autoimmunity, where many potential therapeutic targets are intracellular proteins. As a model, we provide a test of the 3DNA delivery system for siRNA targeted to IDO2 in B cells as a way to ameliorate autoimmune disease. KRN.g7 is a well-characterized T-cell transgenic murine model system that recapitulates the joint inflammation, immune cell infiltrates, and destruction of cartilage and bone characteristic of human RA. We demonstrate successful targeted, low-dose 3DNA-based delivery of siRNA to B cells in this system, mitigating arthritis severity.

Methods

siRNA identification

B cells were purified from spleen tissue harvested from C57BL/6 mice. Tissue was passed through a 70-µm nylon strainer to generate a single-cell suspension. B cells were isolated using negative selection by magnetic purification with CD43 beads (P/N 130-049-801; Miltenyi Biotec, Auburn, CA, USA). B cells (2×10^5) were cultured in 200 µL Iscove's Modified Dulbecco's Medium (IMDM) with 2.5% fetal calf serum (FCS), 5 µM 2-ME, 2 mM glutamax (Life Technologies, Carlsbad, CA, USA), 50 µg/mL gentamicin with 25 µg/mL lipopolysaccharide (LPS) + 5 ng/mL interleukin 4 (IL-4). Dharmacon Accell siRNA (GE Life Sciences, Boston, MA, USA; EQ-053502-00-0002, siRNA 1, 2, 3, and 4 = A-053502-13,-14, -15, and -16, respectively) was added to a final concentration of 100 µM. Cultures were incubated for 72 hours at 37°C with 5% CO_2. RNA was prepared for quantitative real-time PCR (qRT-PCR) with RNeasy Mini Kit (Qiagen, Germantown, MD, USA) according to kit instructions. First-strand cDNA was synthesized using 1:1 random hexamer and oligo-dT primer (Promega GoScript, P/N A5000; Promega, Madison, WI, USA). IDO2 expression was measured by qRT-PCR using SYBR Green (P/N S4428; Sigma-Aldrich, St. Louis, MO, USA). Expression of target gene IDO2 was determined relative to β2-microglobulin (β2M) and calculated as 2^-ΔΔCt (Ct_{IDO2} gene—$Ct\beta_{2M}$) as primers had similar efficiencies. SYBR Green primers for IDO2 were 5′-GCCCAGAGCTCCGTG CTTCAT-3′ and 5′-TGGGAAGGCGGCATGTAGTCC-3′ and for β2M, 5′-CTCGGTGACCCTGGTCTTTC-3′ and 5′-TTGAGGGGTTTTCTGGATAGCA-3′.

3DNA formulations

3DNA was manufactured by Genisphere LLC (Hatfield, PA, USA) in a series of sequential DNA strand hybridization and crosslinking steps to achieve a 2-layer 3DNA configuration. For internalization and biodistribution studies, dye-labeled oligos (AlexaFluor488 or AlexaFluor647) were crosslinked to the 2-layer 3DNA structure, then targeting DNA conjugates were hybridized to the fluorescent 3DNA, to prepare formulations denoted as antibody-3DNA-fluor. Targeting DNA conjugates were prepared with anti-CD19 or Rat IgG2a isotype control antibodies (anti-CD19, clone 1D3, P/N BE0150; isotype control clone 2A3, catalog # BE0089; BioXcell, Lebanon, NH, USA) using LC-SMCC (succinimidyl 4-(N-maleimidomethyl)cyclohexane-1-carboxy-(6-amidocaproate)) crosslinker to attach amine-oligo to tris(2-carboxyethyl)phosphine(TCEP)-reduced antibody via a maleimide to the free thiol group. Anti-CD19 was chosen because of its limited ability to deplete B cells.[37,38] By nucleic acid sequence design, targeting DNA conjugates hybridize 3DNA sequences with a melting temperature (Tm) of 72°C. Hybridization was conducted by incubating at 37°C for 30 minutes using a molar ratio of 0.144:1 conjugate to 3DNA. For siRNA efficacy studies, the 2-layer 3DNA structure was hybridized with modified siRNA and antibody-oligo conjugate to prepare formulations denoted as anti-CD19-3DNA-siIDO2, anti-CD19-3DNA-siControl, and Rat IgG-3DNA-siIDO2. The siRNA oligos were purchased from IDT (Integrated DNA Technologies, Coralville, IA, USA) with bases modified for stability and short DNA extension on

sense strand to hybridize 3DNA (IDO2 target sequence: CCCUCGUCCCUUAGUCUUU; Control target sequence: GUUGCGACUUAUCGUUCGG). Stability modification includes addition of 2′-O-Methyl RNA Bases, 2′ Fluoro Bases, and 2 additional 3′ terminal mU bases, which are commonly added to protect siRNA. By nucleic acid sequence design, DNA-extended and stability-modified siRNA oligos hybridize 3DNA sequences with a Tm of 53°C. Hybridization was conducted by incubating at 37°C for 30 minutes using a molar ratio of 0.524:1 siRNA to 3DNA. All conjugates are purified using thiophilic adsorption chromatography (TAC) to remove unconjugated oligo. In addition, they are purified using a diethylaminoethyl (DEAE) column to remove free antibody.

To test binding of 3DNA, spleen tissue was harvested from C57BL/6 mice. Tissue was passed through a 70-μm nylon strainer to generate a single-cell suspension. Cells were incubated for 15 minutes at 4°C with 0.2 μg αCD19, Rat IgG2a isotype control, oligo-conjugated αCD19, αCD19-3DNA-AlexaFluor647, or αCD19-3DNA-siIDO2. Secondary antibody used for detection of αCD19 or isotype control was anti-rat IgG2a-FITC (clone MRG2a-83 P/N 407505; BioLegend, San Diego, CA, USA). Cells were read on a BD FACSCanto flow cytometer with FACSDiVa software (BD Biosciences, San Jose, CA, USA) and data analyzed with FlowJo software (TreeStar, Ashland, OR, USA).

Internalization

Spleen cells were isolated from C57BL/6 mice as described above, stained on ice with the B-cell marker (B220-eFluor 570, clone RA3-6B2, P/N 41045280; eBioscience, San Diego, CA, USA), and incubated with anti-CD19-3DNA-AlexaFluor488 (or Rat IgG-3DNA-AlexaFluor488) for 1 hour at 37°C to allow for internalization. Cells were fixed (IC Fixation Buffer, P/N 88882388; eBioscience) and subsequently incubated with DRAQ5 (P/N 424101; BioLegend) for nuclear visualization; 20 000 labeled cells were acquired using an Amnis ImageStreamX Mark II imaging cytometer with INSPIRE software and analyzed using IDEAS software (Luminex, Seattle, WA, USA).

Biodistribution

The anti-CD19-3DNA-AlexaFluor647 and Rat IgG-3DNA-AlexaFluor647 formulations were injected intravenously (i.v.) into the retro-orbital sinus of C57BL/6 mice. Mice were bled and spleens collected at 10 and 30 minutes after injection. Blood and spleen cells were stained for the following markers and analyzed by flow cytometry using a BD FACSCanto II and BDFACSDiVa software with subsequent analysis using FlowJo software (TreeStar): B cells (B220-PerCP, clone RA3-6B2, P/N 103234; BioLegend), T cells (CD4-APC-Cy7, clone GK1.5, P/N 100414 + CD8 APC-Cy7, clone 53-6.7, P/N 100714; BioLegend), macrophages (CD11b-FITC, clone M1/70, P/N 101206; BioLegend), and neutrophils (GR-1-PE, clone RB6-8C5, P/N 108408; BioLegend).

To test for 3DNA by PCR, pellets from spleen and peripheral blood lymphocytes (PBLs) injected with dye-labeled 3DNA and isolated as described above were lysed in cell lysis buffer (P/N 9803; Cell Signaling Technology, Danvers, MA, USA) per the manufacturer's instructions. Lysates were similarly obtained from animals with no 3DNA treatment, then spiked with the appropriate 3DNA formulation to prepare standard curves specific for each sample and treatment. Detection of 3DNA in cell lysates was completed using probe-based PCR with primers and probes specific for 3DNA and the Promega GoTaq Probe qPCR Master Mix. Each sample was run in triplicate. Polymerase chain reaction and quantitative analysis were done using ABI 7300 PCR instrument and the system software.

Arthritis incidence

KRN TCR Tg mice on a C57BL/6 background have been described.[39] Arthritic mice were generated by breeding KRN Tg C57BL/6 mice expressing the I-A^{g7} major histocompatibility complex (MHC) class II molecule (KRN.g7). KRN.g7 arthritic mice were injected twice weekly i.v. into the retro-orbital sinus with anti-CD19-3DNA-siIDO2, anti-CD19-3DNA-siControl, or Rat Ig-3DNA-siIDO2 beginning at weaning (3 weeks, just before arthritis onset) until 6 weeks of age and followed for arthritis development. The 2 rear ankles of KRN.g7 mice were measured starting at weaning (3 weeks of age). Measurement of ankle thickness was made above the footpad axially across the ankle joint, using a Fowler Metric Pocket Thickness Gauge (P/N 52-545-001; Fowler High Precision, Newton, MA, USA). Ankle thickness was rounded off to the nearest 0.05 mm. All mice were bred and housed under specific pathogen-free conditions in the animal facility at the Lankenau Institute for Medical Research. Studies were performed in accordance with National Institutes of Health and Association for Assessment and Accreditation of Laboratory Animal Care guidelines with approval from the Lankenau Institute for Medical Research Institutional Animal Care and Use Committee.

Results and Discussion

Nanocarrier formulations

As a strategy to inhibit IDO2 in B cells, we prepared 3DNA nanocarriers targeted with anti-CD19 antibody to deliver siRNA against IDO2. CD19 was chosen as a B-cell-directing target because anti-CD19 antibodies do not cause depletion of conventional splenic B cells on their own,[37] simplifying interpretation of potential therapeutic results. In addition, anti-CD19 Ig has been shown to be readily internalized by B cells in models of lymphoma.[40] Flow cytometric analysis showed equal cell binding of antibody alone and antibody-oligo conjugate,

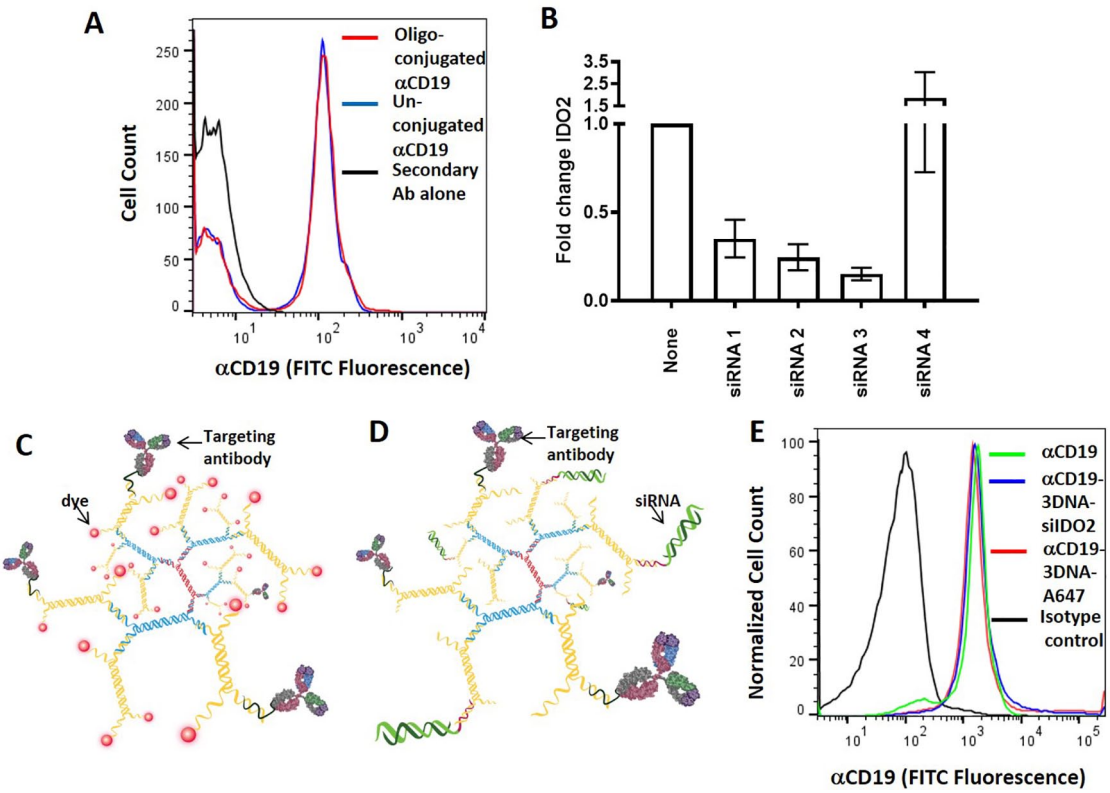

Figure 1. 3DNA components and formulations. (A) Spleen cells from C57BL/6 mice were stained with unconjugated or oligo-conjugated anti-CD19 and examined by flow cytometry. Both unconjugated anti-CD19 and anti-CD19-oligo conjugate showed equal binding, demonstrating the DNA conjugation chemistry did not negatively affect the binding capacity of the antibody. (B) Purified B cells were stimulated with LPS + IL-4 to induce IDO2, transfected with anti-IDO2 siRNA, and IDO2 RNA levels were measured by qRT-PCR. Graphs show mean fold change in IDO2 ± SEM compared with control for n = 3 per condition. (C, D) With both targeting and payload moieties confirmed, 2-layer, 3DNA nanocarrier was then formulated. Representative diagrams of 3DNA targeting constructs were shown. (C) For targeting and biodistribution studies, dye-labeled oligos (red dots) are crosslinked to peripheral 3DNA sequences, while antibody-oligo conjugates (Y-shaped structures) are hybridized to peripheral 3DNA sequences. (D) For therapeutic efficacy studies, modified siRNA oligos (green) and antibody-oligo conjugates are hybridized to their respective complementary peripheral 3DNA sequences. (E) B-cell-binding capacity of 3DNA constructs was compared with the binding capacity of the unconjugated anti-CD19 antibody. B cells are able to bind antibody alone or anti-CD19 hybridized to 3DNA with identical capacity. SEM, standard error of mean.

suggesting the DNA conjugation chemistry did not negatively affect the binding capacity of the antibody (Figure 1A). To identify a suitable anti-IDO2 siRNA, 4 separate commercially available siRNA constructs were first tested in vitro. B cells from C57BL/6 mice were purified and IDO2 induced using LPS + IL-4 as previously described.[13] The 4 siRNAs were then individually transfected into the purified B cells and IDO2 mRNA isolated after 72 hours. Of these, siRNA 3 reduced the measurable level of IDO2 mRNA (Figure 1B) and was used in subsequent 3DNA formulations. To create the nanocarrier itself, unique DNA strands are hybridized to form monomers, which are subsequently assembled and crosslinked into the 3-dimensional structure termed 3DNA. The resulting 2-layer 3DNA scaffold is double-stranded in its core and single-stranded in its peripheral DNA sequences. By design, targeting DNA conjugates are complementary to the 3′-terminal single-stranded sequences of 3DNA, while dye-labeled oligos and/or modified siRNA oligos are complementary to the 5′-terminal 3DNA sequences. For internalization and biodistribution studies, dye-labeled oligos were crosslinked to 3DNA, and antibody-oligo conjugates were hybridized to the fluorescent 3DNA (Figure 1C). For siRNA efficacy studies, modified siIDO2 oligos (or non-specific siControl oligos) and antibody-oligo conjugates were hybridized to unlabeled 3DNA (Figure 1D). To ensure that the anti-CD19-3DNA nanocarrier has the same B-cell-binding capacity as unconjugated antibody, splenocytes were incubated with either anti-CD19 alone or siRNA or dye-labeled anti-CD19-3DNA construct (Figure 1E). No differences were seen in binding capacity of the targeted 3DNA compared with antibody alone.

B cells internalize anti-CD19-3DNA

To determine whether the 3DNA is able to bind to and internalize in B cells, internalization of 3DNA was measured by imaging cytometry. Splenocytes were isolated from C57BL/6 mice, stained with the B-cell marker B220, and incubated with anti-CD19-3DNA-A488 or Rat IgG-3DNA-A488 for 1 hour at 37°C to allow for internalization. Intensity of 3DNA in B cells ($B220^+$) and other splenocytes ($B220^-$) demonstrates that

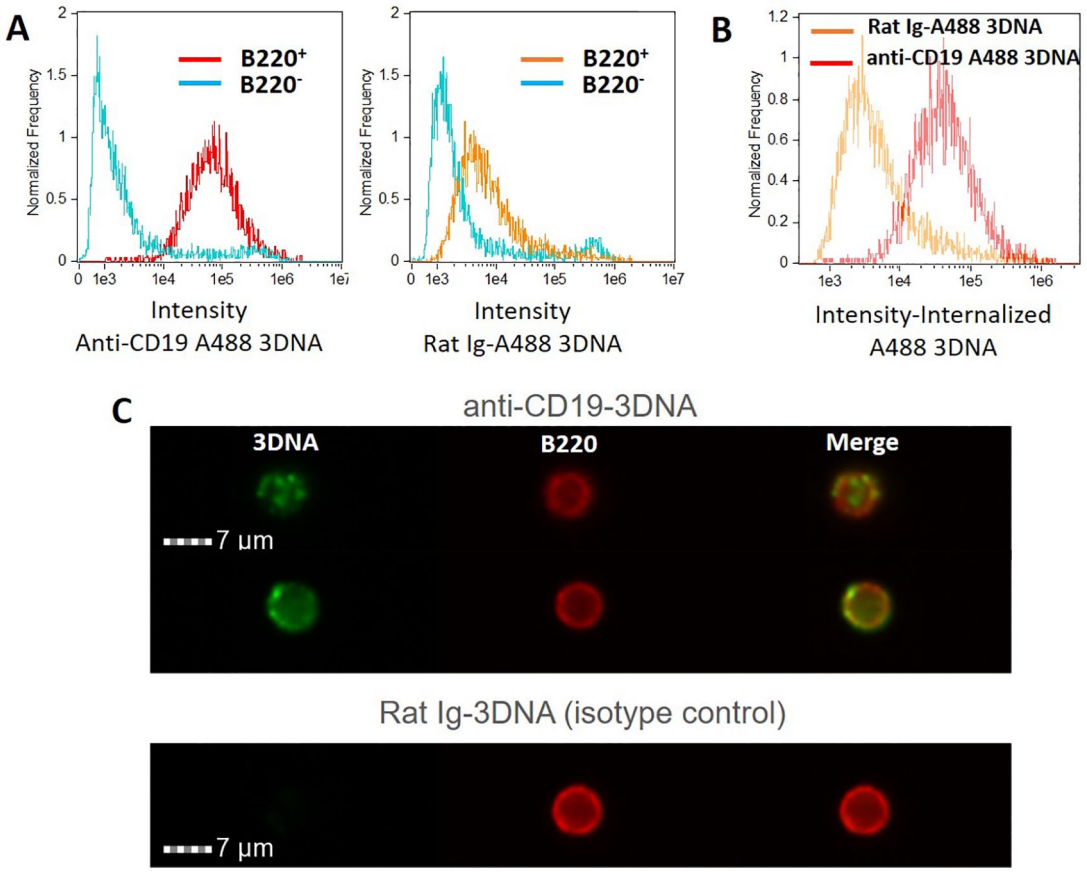

Figure 2. Anti-CD19-targeted 3DNA is internalized in B cells with limited binding of isotype control 3DNA. (A) Anti-CD19-3DNA or Rat Ig-3DNA hybridized with AlexaFluor488 was incubated for 60 minutes at 37°C with spleen cells from C57BL/6 mice and analyzed by imaging cytometry. Anti-CD19 3DNA targets B cells (left panel), while isotype control 3DNA does not (right panel). (B) B220 staining was used to define the cell surface based on Imagestream images. Intensity of internalized anti-CD19 or Rat Ig-3DNA staining defined as the intensity of AlexaFluor488 staining in an area defined as the cell boundary eroded toward the cell center by 4 pixels. (C) Representative images show B220 surface staining (red) and anti-CD19 or isotype control 3DNA (green) on individual cells. A representative experiment of 3 independent trials is shown.

the anti-CD19 3DNA preferentially binds and internalizes to B cells, while isotype-control-hybridized 3DNA does not (Figure 2A). To determine whether the 3DNA actually enters the cell or whether it remains bound on the cell surface, the intensity of internalized 3DNA was determined. Surface B220 staining was used to define the cell membrane and internalized 3DNA defined as intensity of A488 label carried by the 3DNA in an area 4 pixels internal to the defined boundary. We find that substantial anti-CD19 3DNA is found inside the B cells, while little isotype control 3DNA is found inside the cell boundary (Figure 2B and C), indicating that targeting is precise and internalization successful.

Delivery of 3DNA to B cells in vivo

To test delivery to B cells in vivo, biodistribution studies were performed with anti-CD19-3DNA-A647 and Rat IgG-3DNA-A647. Mice were injected with these formulations and blood and spleen taken at 10 and 30 minutes after injection and subsequently analyzed by flow cytometry. At 10 minutes after injection, >90% of B cells in the peripheral blood are labeled with the anti-CD19-3DNA, while most of the B cells do not take up the isotype-control-3DNA (Figure 3A). By 30 minutes, less than 15% of the peripheral blood B cells remain labeled with anti-CD19-3DNA (Figure 3B). This was not because the labeled B cells migrated out of the peripheral blood to the spleen, as the percentage of labeled B cells also decreased in the spleen after 30 minutes (Figure 3C and D). At both 10 and 30 minutes in the peripheral blood and spleen, there is minimal labeling of T cells and, while some neutrophils also have a label, they constitute only a small proportion of total cells and take up both anti-CD19 and isotype control 3DNA equally (Figure 3A-D). Interestingly, almost 50% of macrophages in the spleen and approximately 75% of macrophages in the peripheral blood are labeled with anti-CD19-3DNA by 10 minutes. This is likely due to non-specific engulfment of the 3DNA, as significant percentages of macrophages also label with isotype-control-3DNA. Although some surface binding is clearly present in macrophages, Imagestream data show that little 3DNA is internalized into $B220^-$ cells (Figure 2A). As was seen in the B cells, by 30 minutes, most of the label has disappeared in the macrophages. Thus, the anti-CD19 3DNA is able to rapidly bind and be internalized by the targeted B cells. This targeting is efficient, with over 90%

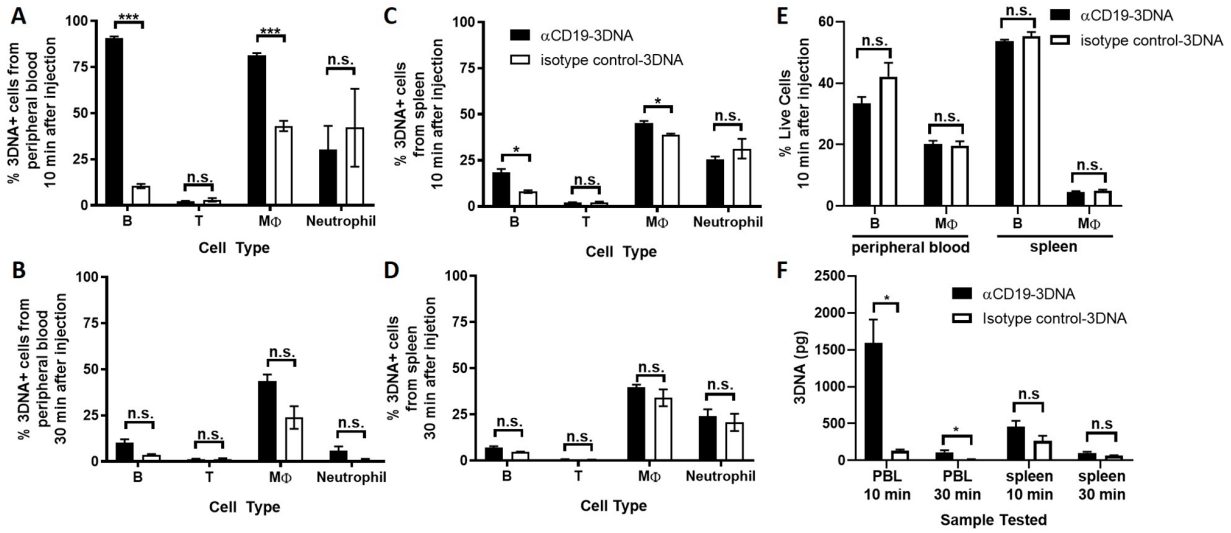

Figure 3. 3DNA rapidly binds to target B cells in vivo. AlexaFluor647-labeled anti-CD19 or isotype control 3DNA was injected intravenously into C57BL/6 mice. Cells from the (A, B) peripheral blood and (C, D) spleen were harvested after (A, C) 10 minutes or (B, D) 30 minutes and analyzed by flow cytometry, with cell type defined with the following markers: B cells (B220), T cells (CD4 + CD8), macrophages (MΦ, CD11b), and neutrophils (GR-1). Graphs show the mean percentage of labeled cells ± SEM for n = 3 mice/group. (E) The proportion of the 2 cell types that primarily bind 3DNA, B cells, and macrophages is shown in the spleen and peripheral blood. Graphs show mean percentage of labeled cells ± SEM for n = 3 to 6 mice/group. (F) 3DNA in peripheral blood and spleen was measured by PCR. Graph shows the mean pg 3DNA ± SEM for n = 3 mice/group. Statistical significance is determined by *t* test with the Holm-Sidak correction for multiple comparisons. $^{*}P < 0.05$; $^{***}P < 0.001$. n.s. indicates not significant; PCR, polymerase chain reaction; SEM, standard error of mean.

of circulating B cells showing binding of CD19-directed 3DNA within the first 10 minutes. The anti-CD19-3DNA does not appear to be toxic to the cells, as no significant differences are seen in the proportion of B cells and macrophages in peripheral blood or spleen when treated with anti-CD19-3DNA compared with isotype control (Figure 3E).

To confirm the presence of 3DNA itself in the target tissues, and to determine whether the label was being rapidly cleaved or the 3DNA itself was being degraded, PCR was performed to test for the presence of a DNA strand unique to the initiating monomer and 2nd layer of the 3DNA structure in whole PBLs and spleen. In agreement with our flow cytometry analysis, distribution to the spleen and peripheral blood is rapid, with much of the 3DNA disappearing by 30 minutes (Figure 3F). This finding suggests the 3DNA delivery system rapidly distributes to the tissues and is quickly broken down following target delivery. This rapid delivery and degradation is important because it indicates that the 3DNA is able to quickly release the therapeutic deliverable to the tissue of interest and that the delivery system itself does not linger in the cell.

Efficacy and dose response of in vivo delivery of siRNA with the 3DNA nanocarrier

Having established that the 3DNA delivery system can be successfully directed to and internalized by B cells, we next examined whether this system could therapeutically deliver siIDO2 to reduce autoimmunity in the KRN.g7 preclinical arthritis model. Previous work has established that reduction in IDO2, either by genetic deletion or antibody therapy, ameliorates arthritis in this system.[12,14,29] To test efficacy of the 3DNA-delivered anti-IDO2 siRNA, mice were dosed with 9.6 µg anti-CD19-3DNA-siIDO2. Control mice were left untreated or received an equal dose of either anti-CD19-siControl or RatIg-3DNA-siIDO2 (Figure 4A). In the KRN.g7 model, mice spontaneously develop arthritis starting at 4 weeks of age, with inflammation peaking around 6 weeks of age.[39,41] Treatment with anti-CD19-3DNA-siIDO2 delayed the time of onset and decreased the overall severity of arthritis (Figure 4A). No effect on arthritis was observed in mice dosed with B-cell (anti-CD19)-directed 3DNA with a non-specific siRNA sequence (anti-CD19-3DNA-siControl). Likewise, IDO2 siRNA formulated with 3DNA molecule not directed to B cells (Rat Ig-3DNA-siIDO2) also did not affect arthritis. Importantly, the anti-CD19-3DNA-siControl and Rat Ig-3DNA-siIDO2 had a course of arthritis similar to untreated controls, indicating that the 3DNA constructs themselves do not provoke any toxicity or anti-CD19 mediated immune suppression that can account for the reduction in arthritis. Thus, the 3DNA approach is able to successfully deliver an efficacious dose of siRNA to B cells, and the therapeutic effect requires both B cell targeting with the anti-CD19 antibody and IDO2 targeting with IDO2-specific siRNA.

Next, we examined the dose response of the siIDO2 3DNA to determine the maximal effect of the anti-IDO2 therapy and to determine the lowest dose that still results in a reduction in arthritis. Three-week-old KRN.g7 mice were dosed with anti-CD19 3DNA hybridized with 1 of 6 doses of anti-IDO2 siRNA (0.013, 0.1, 1.1, 3.2, 9.6, or 28.3 µg; Figure 4B). Increasing the siIDO2 dose to 28.3 µg did not provide a

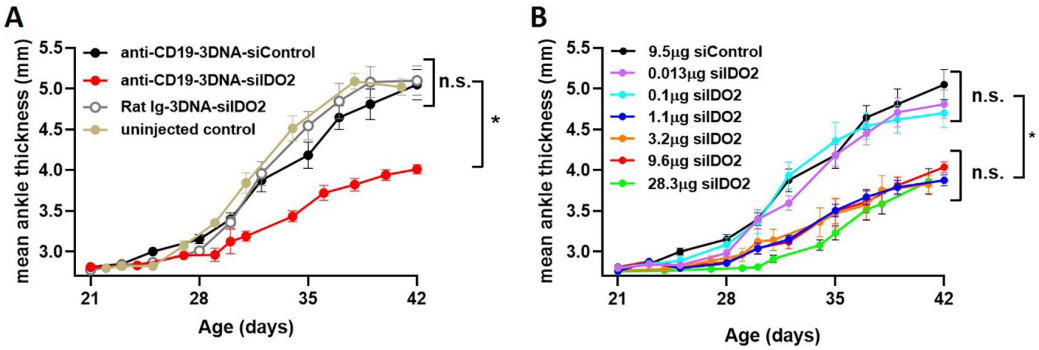

Figure 4. Anti-CD19-3DNA-siIDO2 inhibits arthritis in a preclinical model. KRN.g7 mice were treated 2 times per week beginning at weaning (3 weeks of age) with (A) 9.6 μg anti-CD19-3DNA-siIDO2, anti-CD19-3DNA-siControl, Rat Ig-3DNA-siIDO2, or untreated control and (B) a dose response of siIDO2. Dose of IDO2 was determined by formulations of 0.013 to 28.3 μg siIDO2 with anti-CD19 3DNA. Anti-CD19-3DNA-siIDO2 (red) and anti-CD19-siControl (black) (9.6 μg) from panel (A) are shown again in panel (B) for comparison. Graphs show the mean ankle thickness ± SEM for n = 4 to 8 mice/group. Statistical significance was determined by 1-way ANOVA with post hoc testing with the Tukey correction for multiple comparisons. *$P < 0.05$. n.s., not significant; SEM, standard error of mean.

therapeutic effect beyond that seen with the 9.6 μg dose. Reducing the siIDO2 dose to as low as 1.1 μg still provided the same therapeutic effect as higher doses. However, the therapeutic effect was lost when the dosage was lowered to 0.1 μg (Figure 4B). Interestingly, the inhibition of IDO2 seems to give an "all-or-none" response rather than a reduction in arthritis relative to dosage: at 1.1 μg and above, arthritis was reduced and there was no additional effect seen by giving more siIDO2. Given an average mouse weight of 12 g at Day 21 and 20 g at Day 42, the corresponding efficacious siRNA dose ranges from ~0.055 to ~2.3 mg/kg, in line with existing FDA-approved siRNA therapies ONPATTRO (patisiran, 0.3 mg/kg) and GIVLAARI (givosiran, 2.5 mg/kg).[42] This strong biological response seen at a very low dose of siIDO2 highlights the benefit of precise targeting with the B-cell-directed 3DNA. Without targeting, there is no activity of the siRNA, indicating the importance of mitigating the effect of IDO2 in B cells as a mechanism of arthritis reduction and the effective dose delivery by this nanotherapy system.

Summary

Many promising therapeutic targets are difficult to reach due to their lack of surface expression or the difficulty in targeting specific cell types for therapy. 3DNA nanotechnology can overcome these challenges, providing a rapid and effective method for targeting specific cell types with a variety of potential therapies, including small molecule cytotoxic compounds, antibodies, or siRNAs.

This work provides a direct in vivo test of the efficacy of 3DNA as a delivery vehicle for autoimmune therapies. The versatility of this technology opens up a world of targets, including applications where small molecule inhibitors are lacking and direct antibody targeting is not possible. While the studies here provide a proof of concept for siRNA delivery, this technology has the potential to be used for efficient delivery of multiple therapy types directed to specific cells, thereby bypassing toxicity issues associated with off-target effects and, because of the exquisitely targeted approach, requiring lower doses of drugs, antibodies, or siRNAs, thereby reducing side effects.

Author Contributions

L.M.-N. directed the work and oversaw the planning and implementation of experiments described, and conducted in vivo arthritis experiments. L.M.-N. and L.M.F.M. performed biodistribution studies. L.M.F.M. designed and performed in vitro analysis of siRNA and internalization studies, and also prepared the manuscript. T.S. performed quantitative analysis of 3DNA in peripheral blood and spleen by PCR. J.B. and R.G. oversaw design and formulation of 3DNA reagents. All authors contributed to the manuscript revision, and read and approved the submitted version.

ORCID iDs

Lauren MF Merlo https://orcid.org/0000-0002-5244-6448
Laura Mandik-Nayak https://orcid.org/0000-0001-9030-3467

REFERENCES

1. Hayter SM, Cook MC. Updated assessment of the prevalence, spectrum and case definition of autoimmune disease. *Autoimmun Rev*. 2012;11:754-765.
2. Walsh SJ, Rau LM. Autoimmune diseases: a leading cause of death among young and middle-aged women in the United States. *Am J Public Health*. 2000;90:1463-1466.
3. Rosenblum MD, Gratz IK, Paw JS, Abbas AK. Treating human autoimmunity: current practice and future prospects. *Sci Transl Med*. 2012;4:125sr1.
4. Helmick CG, Felson DT, Lawrence RC, et al. Estimates of the prevalence of arthritis and other rheumatic conditions in the United States. Part I. *Arthritis Rheum*. 2008;58:15-25.
5. Gibofsky A. Epidemiology, pathophysiology, and diagnosis of rheumatoid arthritis: a synopsis. *Am J Manag Care*. 2014;20:S128-S135.
6. Birnbaum H, Pike C, Kaufman R, Marynchenko M, Kidolezi Y, Cifaldi M. Societal cost of rheumatoid arthritis patients in the US. *Curr Med Res Opin*. 2010;26:77-90.
7. Curtis JR, Singh JA. Use of biologics in rheumatoid arthritis: current and emerging paradigms of care. *Clin Ther*. 2011;33:679-707.
8. Singh JA, Furst DE, Bharat A, et al. 2012 update of the 2008 American College of Rheumatology recommendations for the use of disease-modifying antirheumatic drugs and biologic agents in the treatment of rheumatoid arthritis. *Arthritis Care Res (Hoboken)*. 2012;64:625-639.
9. Alghasham A, Rasheed Z. Therapeutic targets for rheumatoid arthritis: progress and promises. *Autoimmunity*. 2014;47:77-94.

10. Singh JA, Saag KG, Bridges SL Jr, et al. 2015 American College of Rheumatology guideline for the treatment of rheumatoid arthritis. *Arthritis Rheumatol*. 2016;68:1-26.
11. Smolen JS, Steiner G. Therapeutic strategies for rheumatoid arthritis. *Nat Rev Drug Discov*. 2003;2:473-488.
12. Merlo LM, Pigott E, DuHadaway JB, et al. IDO2 is a critical mediator of autoantibody production and inflammatory pathogenesis in a mouse model of autoimmune arthritis. *J Immunol*. 2014;192:2082-2090.
13. Merlo LM, DuHadaway JB, Grabler S, Prendergast GC, Muller AJ, Mandik-Nayak L. IDO2 modulates T cell-dependent autoimmune responses through a B cell-intrinsic mechanism. *J Immunol*. 2016;196:4487-4497.
14. Merlo LM, Mandik-Nayak L. IDO2: a pathogenic mediator of inflammatory autoimmunity. *Clin Med Insights Pathol*. 2016;9:21-28.
15. Muller AJ, Prendergast GC. Indoleamine 2,3-dioxygenase in immune suppression and cancer. *Curr Cancer Drug Targets*. 2007;7:31-40.
16. Prendergast GC. Immune escape as a fundamental trait of cancer: focus on IDO. *Oncogene*. 2008;27:3889-3900.
17. Prendergast GC, Chang MY, Mandik-Nayak L, Metz R, Muller AJ. Indoleamine 2,3-dioxygenase as a modifier of pathogenic inflammation in cancer and other inflammation-associated diseases. *Curr Med Chem*. 2011;18:2257-2262.
18. Munn DH. Blocking IDO activity to enhance anti-tumor immunity. *Front Biosci (Elite Ed)*. 2012;4:734-745.
19. Gurtner GJ, Newberry RD, Schloemann SR, McDonald KG, Stenson WF. Inhibition of indoleamine 2,3-dioxygenase augments trinitrobenzene sulfonic acid colitis in mice. *Gastroenterology*. 2003;125:1762-1773.
20. Sakurai K, Zou JP, Tschetter JR, Ward JM, Shearer GM. Effect of indoleamine 2,3-dioxygenase on induction of experimental autoimmune encephalomyelitis. *J Neuroimmunol*. 2002;129:186-196.
21. Szanto S, Koreny T, Mikecz K, Glant TT, Szekanecz Z, Varga J. Inhibition of indoleamine 2,3-dioxygenase-mediated tryptophan catabolism accelerates collagen-induced arthritis in mice. *Arthritis Res Ther*. 2007;9:R50.
22. Ravishankar B, Liu H, Shinde R, et al. Tolerance to apoptotic cells is regulated by indoleamine 2,3-dioxygenase. *Proc Natl Acad Sci USA*. 2012;109:3909-3914.
23. Xu H, Oriss TB, Fei M, et al. Indoleamine 2,3-dioxygenase in lung dendritic cells promotes Th2 responses and allergic inflammation. *Proc Natl Acad Sci USA*. 2008;105:6690-6695.
24. von Bubnoff D, Bieber T. The indoleamine 2,3-dioxygenase (IDO) pathway controls allergy. *Allergy*. 2012;67:718-725.
25. Metz R, Smith C, DuHadaway JB, et al. IDO2 is critical for IDO1-mediated T cell regulation and exerts a non-redundant function in inflammation. *Int Immunol*. 2014;26:357-367.
26. Put K, Brisse E, Avau A, et al. IDO1 deficiency does not affect disease in mouse models of systemic juvenile idiopathic arthritis and secondary hemophagocytic lymphohistiocytosis. *PLoS ONE*. 2016;11:e0150075.
27. Liu X, Shin N, Koblish HK, et al. Selective inhibition of IDO1 effectively regulates mediators of antitumor immunity. *Blood*. 2010;115:3520-3530.
28. Sheridan C. IDO inhibitors move center stage in immuno-oncology. *Nat Biotechnol*. 2015;33:321-322.
29. Merlo LMF, Grabler S, DuHadaway JB, et al. Therapeutic antibody targeting of indoleamine-2,3-dioxygenase (IDO2) inhibits autoimmune arthritis. *Clin Immunol*. 2017;179:8-16.
30. Wittrup A, Lieberman J. Knocking down disease: a progress report on siRNA therapeutics. *Nat Rev Genet*. 2015;16:543-552.
31. Muro S. A DNA-device that mediates selective endosomal escape and intracellular delivery of drugs and biologicals. *Adv Funct Mater*. 2014;24:2899-2906.
32. Roki N, Tsinas Z, Solomon M, Bowers J, Getts RC, Muro S. Unprecedently high targeting specificity toward lung ICAM-1 using 3DNA nanocarriers. *J Control Release*. 2019;305:41-49.
33. Huang YH, Peng W, Furuuchi N, et al. Delivery of therapeutics targeting the mRNA-binding protein HuR using 3DNA nanocarriers suppresses ovarian tumor growth. *Cancer Res*. 2016;76:1549-1559.
34. Gerhart J, Greenbaum M, Casta L, et al. Antibody-conjugated, DNA-based nanocarriers intercalated with doxorubicin eliminate myofibroblasts in explants of human lens tissue. *J Pharmacol Exp Ther*. 2017;361:60-67.
35. Gerhart J, Werner L, Mamalis N, et al. Depletion of Myo/Nog cells in the lens mitigates posterior capsule opacification in rabbits. *Invest Ophthalmol Vis Sci*. 2019;60:1813-1823.
36. Van Steenwinckel J, Schang AL, Krishnan ML, et al. Decreased microglial Wnt/beta-catenin signalling drives microglial pro-inflammatory activation in the developing brain. *Brain*. 2019;142:3806-3833.
37. Yazawa N, Hamaguchi Y, Poe JC, Tedder TF. Immunotherapy using unconjugated CD19 monoclonal antibodies in animal models for B lymphocyte malignancies and autoimmune disease. *Proc Natl Acad Sci USA*. 2005;102:15178-15183.
38. Keren Z, Naor S, Nussbaum S, et al. B-cell depletion reactivates B lymphopoiesis in the BM and rejuvenates the B lineage in aging. *Blood*. 2011;117:3104-3112.
39. Kouskoff V, Korganow AS, Duchatelle V, Degott C, Benoist C, Mathis D. Organ-specific disease provoked by systemic autoimmunity. *Cell*. 1996;87:811-822.
40. Raufi A, Ebrahim AS, Al-Katib A. Targeting CD19 in B-cell lymphoma: emerging role of SAR3419. *Cancer Manag Res*. 2013;5:225-233.
41. Kyburz D, Corr M. The KRN mouse model of inflammatory arthritis. *Springer Semin Immunopathol*. 2003;25:79-90.
42. Saw PE, Song EW. siRNA therapeutics: a clinical reality. *Sci China Life Sci*. 2020;63:485-500.